Available online at www.sciencedirect.com
ScienceDirect
Deep-Sea Research II 54 (2007) 1312–1326
DEEP-SEA RESEARCH PART II
www.elsevier.com/locate/dsr2

Oxidation of detrital pyrite as a cause for Marcasite Formation in marine lag deposits from the Devonian of the eastern US

Juergen Schieber

Department of Geological Sciences, Indiana University, Bloomington, IN 47405, USA

Accepted 14 April 2007
Available online 10 July 2007

Abstract

Late Devonian black shale successions in the eastern US contain numerous discontinuities that are characterized by lags containing variable amounts of quartz sand mixed with reworked pyritic and phosphatic debris. These lags can be partially cemented by iron sulfides with a radial fibrous to massive morphology. Examination of iron sulfide cements via electron backscatter diffraction (EBSD) shows that these cements can consist entirely or partially of marcasite. It is proposed here that oxidation and dissolution of reworked pyrite debris led to favorable conditions for intermittent rapid marcasite formation by forcing a substantial pH drop in the surface sediment and by raising dissolved iron concentrations in the pore waters.

Keywords: Pyrite; Marcasite; Sequence boundary; Erosion; Oxidation; Black shale

1. Introduction

Flooding surfaces and sequence boundaries in marine mudstone successions, although of subtle expression in many cases, are marked by an increase in authigenic and biogenic components in association with evidence of condensation and/or winnowing (Bohacs, 1998; Schieber, 1998a). The deposits described in this study are lag deposits with variable amounts of phosphatic debris, sand size detrital quartz grains, calcareous shell material, and aggregates of early diagenetic minerals (pyrite, calcite, siderite, chert, etc.). Thin lag deposits with abundant reworked pyrite and phosphatic debris are also found at many discontinuities in other Paleozoic marine shale successions (Baird and Brett, 1991). Because pyrite is liable to be altered to iron oxides when in contact with oxygenated bottom waters, the latter authors proposed that preservation of pyritic lags requires anoxic bottom waters and proposed submarine erosion during sea-level rise by internal waves traveling along the dysoxic/anoxic boundary layer (pycnocline). While the model proposed by Baird and Brett (1991) appears consistent with observed stratal patterns of erosion for the examples that they illustrate, other pyritic lag deposits apparently formed during sea-level drop and without the benefit of internal wave erosion and anoxic bottom waters (Schieber and Riciputi, 2004).

Here I present evidence of early diagenetic marcasite formation in pyritic lag deposits previously studied by Baird and Brett (1991) and by myself (Schieber, 1998a, b; Schieber and Riciputi, 2004). The examined occurrences include the

E-mail address: jSchiebe@Indiana.edu

0967-0645/$ - see front matter © 2007 Published by Elsevier Ltd.
doi:10.1016/j.dsr2.2007.04.005

Leicester Pyrite Member (Baird and Brett, 1991) of the Givetian Geneseo Shale of New York State and three examples from sequence boundaries in the New Albany Shale of Kentucky and Indiana. In all instances marcasite was initially detected on the basis of crystal morphology, and its actual presence was subsequently verified through in situ application of electron backscatter diffraction (EBSD) with a scanning electron microscope.

There are several compelling reasons to understand better the occurrence and formation of early diagenetic marcasite in marine sediments. First, although it presumably should not form in marine sediments during early diagenesis (e.g., Rickard et al., 1995), it nonetheless does. Second, marcasite requires a distinctly lower pH for its formation than pyrite. Third, processes that might produce the necessary low pH values in marine sediments (e.g., re-oxidation of sulfides) are at odds with our concepts about the deposition of the rocks we find associated with it (the enclosing black shales are typically thought of as forming in anoxic/euxinic settings).

Marcasite (FeS_2, orthorhombic) is a dimorph of pyrite (FeS_2, cubic), and just like pyrite it is observed as a diagenetic mineral in sedimentary rocks. Yet, unlike pyrite, it usually is not the focus of sedimentologic investigations, and at best is recorded as a footnote without much detail. Wilkin (2003) summarized the current state of our knowledge in the latest edition of the Encyclopedia of Sediments and Sedimentary Rocks: "Marcasite has not been identified in modern sedimentary environments but is present in some ancient sedimentary rocks". The textural observations presented here suggest that oxidation of pyritic lags is one way in which intermittent marcasite formation in the marine rock record is possible.

2. Methods

Samples from the Late Devonian New Albany Shale in Kentucky and Indiana (Schieber and Lazar, 2004) were collected from outcrops and drill cores and studied with a binocular microscope. Polished thin sections were prepared from iron sulfide-rich samples and studied with reflected-light microscopy and scanning electron microscope (FEI Quanta 400 FEG, located at IU Department of Geological Sciences).

SEM examination included textural studies, energy-dispersive X-ray microanalysis (EDS), and phase identification via EBSD. In EBSD, a stationary electron beam strikes a tilted mineral surface and the diffracted electrons form line patterns (Kikuchi patterns) on a fluorescent screen. These patterns are characteristic of the crystal structure of a given mineral (Prior et al., 1999; Schwartz et al., 2000), and allow phase identification for mineral grains of submicron size, as well as measurement of crystallographic orientation. The EBSD detector used was the Nordlys detector by HKL Technology, and data analysis was conducted with the Channel 5 software package by HKL Technology.

3. Observations

The Late Devonian of the eastern US is largely a black shale-dominated succession (Schieber and Lazar, 2004) that contains a large number of disconformities with lag deposits. These lags contain variable amounts of iron sulfides and four examples that range in age from Givetian to Famennian were chosen to illustrate common themes observed in the iron sulfides of these lags.

3.1. Leicester Pyrite Bed

The first example, the Leicester Pyrite Bed, occurs at the contact between the Tully Limestone and the overlying Geneseo black shale in New York State and consists of lenses of pyritic clasts admixed with quartz grains and phosphatic debris (Baird and Brett, 1991). Reworking of pyrite grains, such as pyritized tubes, nodules, and steinkerns, is indicated by comparison with underlying sediments, current alignment of elongate particles, hydraulic sorting (upward fining), randomizing of geopetal features, and mechanical breakage surfaces (Baird and Brett, 1991).

Examination under reflected light shows that detrital pyrite grains often consist of a mixture of framboidal pyrite with a coarser pyrite cement (Fig. 1A). Many of these grains are overgrown with radiating, blade-shaped crystals (Fig. 1B) of iron sulfide that may show bireflectance and anisotropy when the stage is rotated. The latter properties suggest that the blade-shaped crystals are not pyrite, but rather its dimorph marcasite. EDS analysis under the SEM confirms that all the highly reflective minerals are iron sulfides. EBSD analysis of blade-shaped crystals confirms that they can consist almost entirely of marcasite. In most instances these crystals also contain variable amounts of pyrite

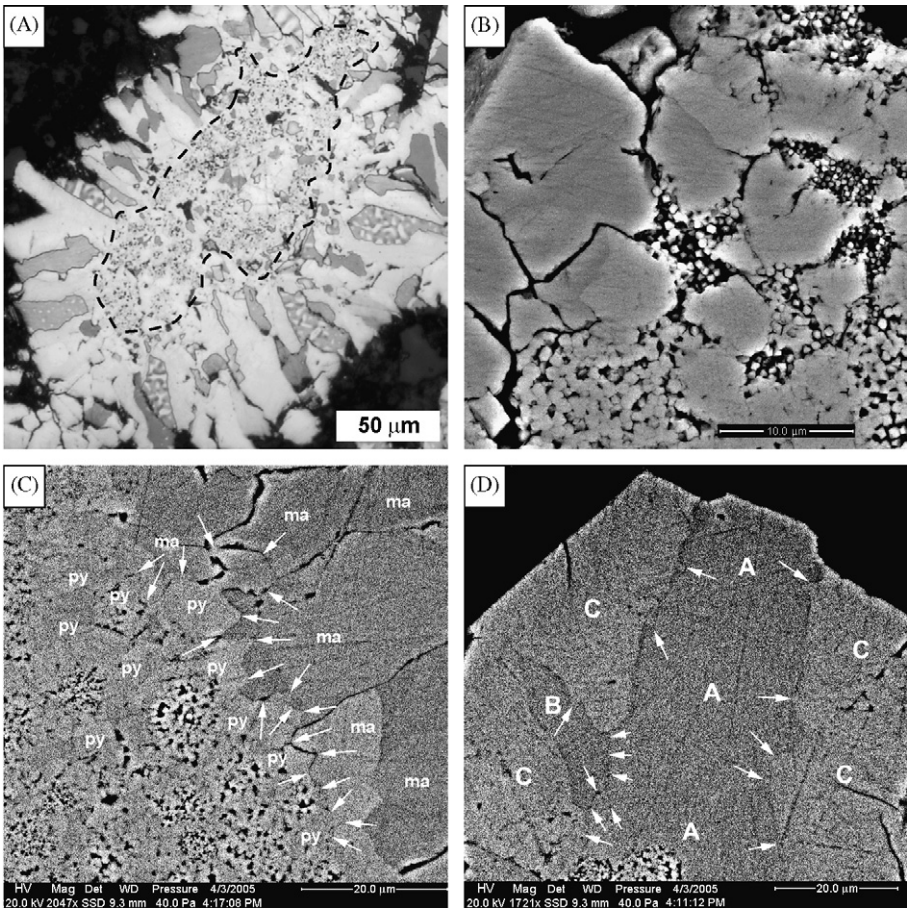

Fig. 1. Petrographic observations from the Leicester Pyrite. (A) detrital core of pyrite grain outlined with dashed black line (reflected light image). Bireflectance of radiating crystals indicates that these consist of marcasite. (B) Edge of iron sulfide grain with framboidal pyrite (clusters of tiny crystals) cemented and overgrown by coarse marcasite (SEM image). The clusters of tiny pyrite crystals near the margin are probably former framboids. Their irregular outlines are attributed to partial dissolution of pyrite prior to marcasite growth. (C) Contact between detrital pyrite grain (py) and marcasite (ma) overgrowth (SEM backscatter image). Orientation contrast imaging causes the different gray shades of adjacent pyrite and marcasite grains. White arrows point to the irregular corroded contact between pyrite and marcasite. (D) Marcasite at the edge of an overgrown reworked pyrite grain (SEM backscatter image). Framboids at the bottom of the image belong to detrital core. We can see a succession of three marcasite generations. Marcasite A grew first on the detrital core. The irregular contact between marcasite A and B (marked by small white arrows) indicates that marcasite B grew on top of A after a dissolution episode caused some corrosion. The fact that there is an irregular and most likely corrosive contact between marcasite B and C suggests yet another episode of dissolution prior to growth of marcasite B. The corrosive contact between marcasite A and C is marked with larger white arrows.

(5–95%), but complete inversion to pyrite has not been observed. Especially at the margins of detrital pyrite grains, the originally round pyrite framboids look distorted, suggestive of possible dissolution of portions of these framboids (Fig. 1B). Closeups of detrital pyrite grains also show features that suggest that corrosion/dissolution of pyrite cement took place prior to overgrowth with marcasite (Fig. 1C). In places it is also possible to document multiple episodes of corrosion and dissolution of marcasite (Fig. 1D).

3.2. Basal Blocher lag

This lag marks a disconformity at the base of the Givetian–Frasnian Blocher Member of the New Albany Shale in Kentucky and Tennessee (Schieber and Lazar, 2004). In many places it marks the contact between Middle Devonian carbonates and overlying black shales of the Blocher Member, is lenticular in nature and ranges in thickness from 0.5 to 5 cm. Variable amounts of reworked pyritic grains are mixed with carbonate grains (carbonate

clasts, crinoid stems, brachiopod shells, etc.) and some phosphatic debris. Detrital pyritic grains (0.05–0.5 mm in size) usually consist of pyrite framboids that are cemented by coarser crystalline pyrite. In pore spaces needle-like iron sulfide grains (EDS analysis) can be found in a cement of calcite and/or dolomite grains (Fig. 2A). EBSD analysis identified many of these needle-like iron sulfides as largely marcasite, with variable portions that had inverted to pyrite. Portions of the lag consist up to 70% or more of iron sulfides in massive aggregates of intergrown pyrite and marcasite (Fig. 2B) due to complete or partial replacement of carbonate grains (Fig. 2C). Within these aggregates, marcasite grains are conspicuous due to their euhedral outlines and elongate-prismatic morphology (Fig. 2C). When examined in detail, the contacts between detrital pyritic grains and marcasite tend to be irregular (Fig. 2D), giving the impression of pyrite dissolution/corrosion prior to marcasite formation.

3.3. Basal Morgan Trail lag

This lag marks the Frasnian/Fammenian boundary in Kentucky and Tennessee (Schieber and Lazar, 2004). It is lenticular in nature, ranges in thickness from 0.5 to 5 cm, and consists of a mixture of rounded quartz sand grains, bone fragments, and detrital pyrite grains (small concretions, fragments of pyritic burrows, etc.). In places the entire pore volume

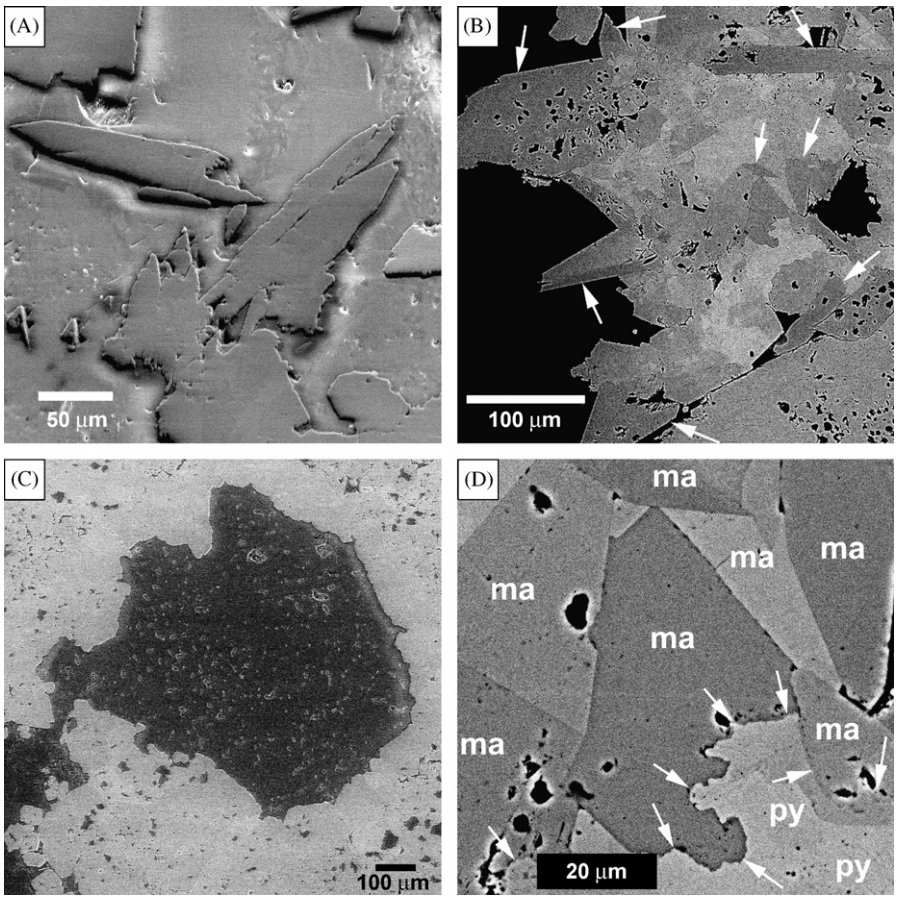

Fig. 2. Petrographic observations from the basal Blocher lag in Harrison County, Indiana (Wiseman #1 well). (A) Pore space that shows needle to blade-shaped marcasite crystals in a carbonate mineral matrix (SEM image). Shows spearhead twins, a typical marcasite morphology. Iron sulfide crystals are still largely marcasite (verification with EBSD). (B) Area with massive iron sulfide growth. Orientation contrast imaging (SEM backscatter) highlights pyrite and marcasite grains (elongate pointed grains, white arrows) through different gray shades. (C) Remnant of carbonate grain (center) that has been partially replaced by marcasite. (D) Detail from image B. Shows contact between detrital pyrite (py) and marcasite (ma) overgrowth. Arrows point out irregular, corroded looking, pyrite–marcasite contact. Orientation contrast imaging (SEM backscatter) highlights euhedral marcasite overgrowth grains (ma) through different gray shades. Marcasite verified with EBSD.

can be filled with iron sulfides (Fig. 3A), whereas other pore spaces are filled with silica cement and/or fine detrital matrix, and iron sulfides (Fig. 3B). Detrital pyrite grains are typically overgrown with radial-bladed iron sulfide crystals (Fig. 3C) that have marcasite morphology and still largely consist of marcasite (verified by EBSD). Pits on the surface of detrital pyrite grains (Fig. 3D) are suggestive of pyrite dissolution prior to marcasite deposition. In places, corroded and partially dissolved marcasite crystals have been observed as well.

3.4. Upper Clegg Creek lag

This is a thin lenticular lag, typically less than 10 mm thick, that occurs in the Clegg Creek Member of the New Albany Shale (Schieber and Lazar, 2004). It consists largely of a mixture of pyrite grains and phosphatic debris that have been reworked from underlying shales (Fig. 4A). Fragments of detrital pyrite that consist of framboidal pyrite cemented by coarser blocky pyrite (Fig. 4B) are overgrown by coarse euhedral iron sulfide crystals. These iron sulfides show bireflectance and anisotropy in reflected light (Fig. 4C). They were examined with EBSD and consist in large parts still of original marcasite. Only small portions (10–20%) have inverted to pyrite. Smaller clusters show the typical radiating habit of marcasite (Fig. 4D). Bone fragments show variable degrees of replacement by iron sulfides.

4. Commonalities

All of these iron sulfide-rich beds overlie erosive surfaces and consist of detrital components that

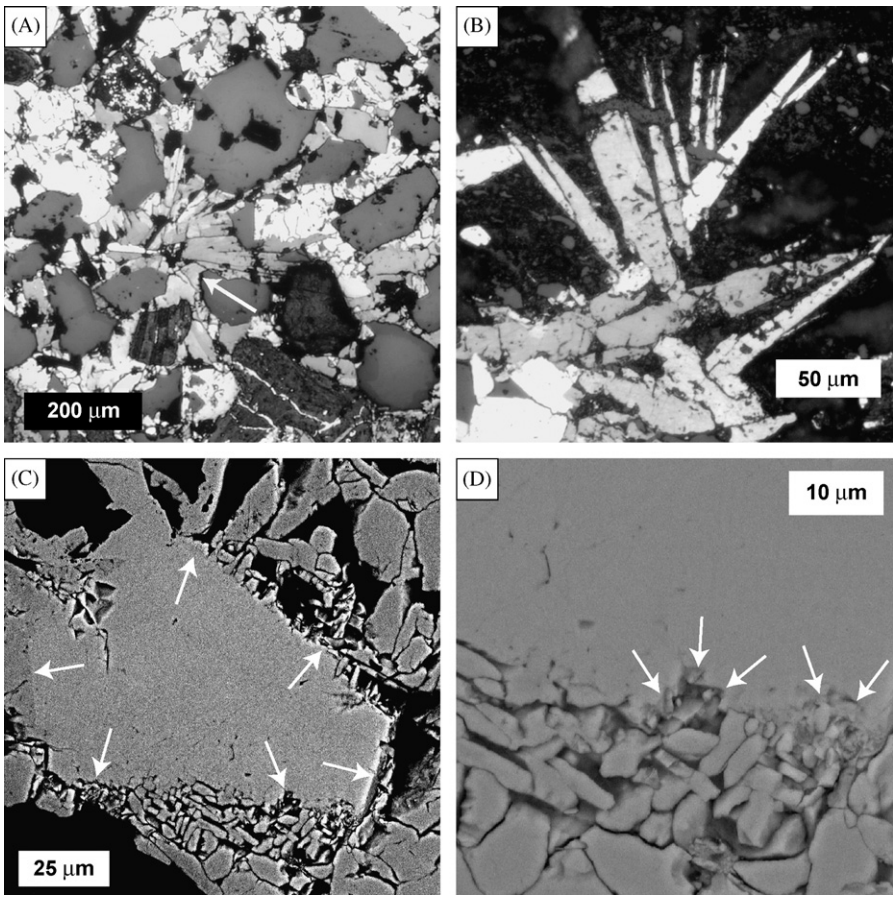

Fig. 3. Petrographic observations from the basal Morgan Trail lag in western Kentucky. (A) Detrital quartz grains with pore filling iron sulfide cement. Arrow points to radial cluster of marcasite (shows bireflectance, reflected light). (B) Pore space with sharp-pointed bireflectant marcasite crystals with spearhead twinning (reflected light). (C) Detrital pyrite grain (marked with white arrows) that is overgrown by bladed marcasite crystals (verified with EBSD). (D) Close-up of grain boundary from previous picture. Shows textural contrast between detrital pyrite grain (upper half) and marcasite overgrowth (lower half). Arrows point out etch pits with marcasite fill.

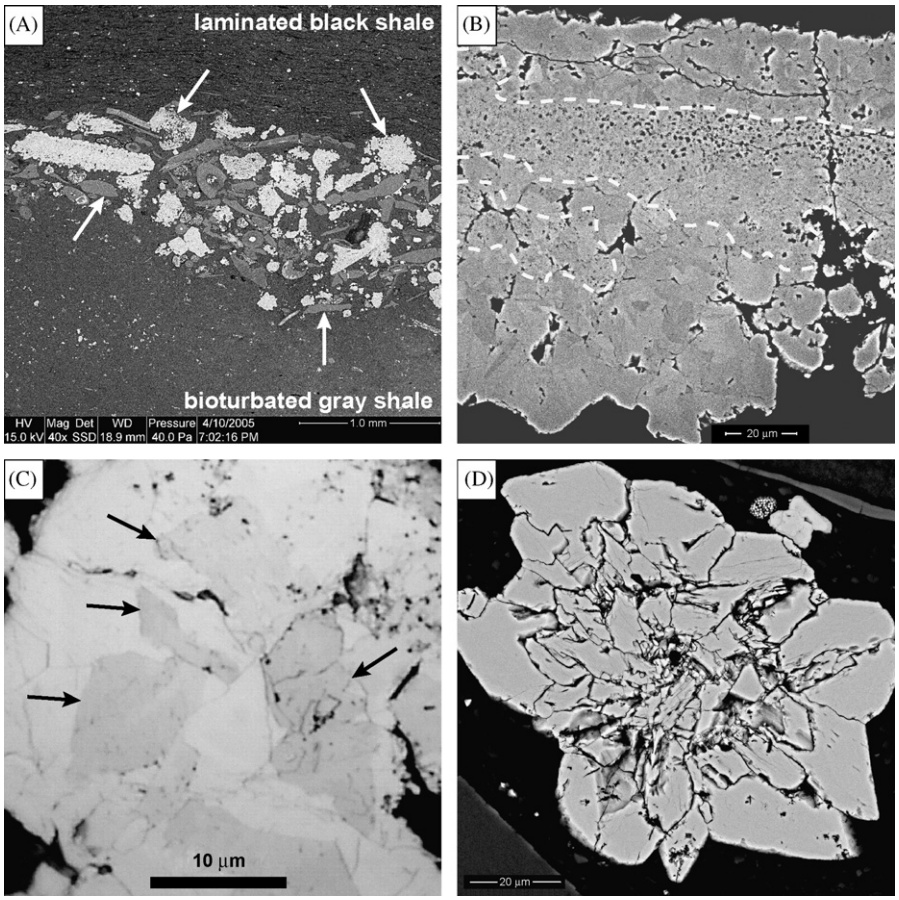

Fig. 4. Petrographic observations from lag in Clegg Creek Member. (A) The lag at the boundary between bioturbated gray shale (below) and laminated black shale. Shows predominance of pyritic (bright white, white arrows) and phosphatic grains (conodonts, fish bone fragments, etc., light gray arrows). (B) Pyrite–marcasite aggregate. Areas of mainly detrital pyrite (framboids and cement) are marked by dashed white lines. Orientation contrast imaging (SEM backscatter) highlights overgrowth rims of interlocking euhedral marcasite (verified by EBSD) through different gray shades. (C) Reflected light image that shows the bireflectance (arrows) typically associated with marcasite. (D) SEM image of small cluster of radiating marcasite (verified by EBSD).

have been reworked from underlying sediments, such as quartz sand grains, phosphatic debris (fish bone fragments, conodonts, *Lingula* shells, etc.), and pyritic grains (concretions, mineralized burrows, pyritized fossils, etc.). The presence of marcasite is indicated by morphological features (radiating fibrous-bladed crystals, spearhead twins), but not all marcasite shows diagnostic morphology. Although more than 350 million years have passed since marcasite formation, measurement of EBSD diffraction patterns confirms that much of this marcasite has not reverted to pyrite. Corrosion textures on detrital pyrite grains suggest that marcasite growth was preceded by partial dissolution of detrital pyrite grains. Associated replacement of carbonate and phosphatic grains by iron sulfides suggests acidic pore waters. There are also indications of subsequent partial dissolution of marcasite and of multiple episodes of iron sulfide dissolution (Fig. 1D).

5. Marcasite in marine sediments

Reports of marcasite in terrigenous clastics are mainly found in association with coal deposits (Nayar, 1946; Read and Cook, 1969; Wiese et al., 1987). There they tend to occur either in the coal seams themselves, or in the roof shales immediately above coal seams. This association, in addition to a presumed requirement for "acidity" based on marcasite occurrences in weathering zones of sulfide deposits (e.g., Newhouse, 1925; Foslie, 1950)

prompted Krumbein and Garrels (1952) to propose an acidic bog/peat association as the characteristic environment for sedimentary marcasite formation. Using similar reasoning, the alkaline pH of seawater was thought to preclude early diagenetic marcasite formation in marine sediments (Rickard et al., 1995). There have, however, been a sufficient number of diagenetic marcasite occurrences reported from normal marine sediments (Maynard and Lauffenburger, 1978; Siesser, 1978; Rykart, 1983; Jowett et al., 1991; Schieber, 2002; Williams et al., 2003), as well as examples of marine marcasite that has inverted to pyrite (Bannister, 1932; Van Horn & Van Horn, 1933), to suggest that it might well be more widespread in the marine realm than commonly appreciated.

6. Original pyrite grains and iron enrichment by surficial reworking

Sedimentary pyrite forms when bacterial sulfate production provides sulfide ions (HS^- and H_2S) that react with dissolved iron to form pyrite either directly or via an iron monosulfide precursor (Berner, 1984; Schoonen, 2004). In most sediments this typically leads to the formation of pyrite framboids, clusters of submicron pyrite crystals that may measure from a few to several tens of microns in diameter (Wilkin and Barnes, 1997). The Devonian black shales within which the lag deposits discussed in this contribution occur contain abundant pyrite framboids (Schieber et al., 1998, 2001), as well as variable amounts of pyritized burrow tubes (Baird and Brett, 1991; Schieber, 2003), pyrite-filled algal cysts (Schieber and Baird, 2001), and irregular pyrite concretions that range in size from a few millimeters to several centimeters.

Studies of modern environments show that pyrite framboids form immediately beneath the redox boundary, be it within the sediment or within the water column in the case of euxinic conditions (Wilkin et al., 1996). In the latter case the framboids can only grow to a size of a few microns before they sink to the seafloor, whereas they reach larger sizes and show a broader size distribution if they grow within the sediment during early diagenesis (Wilkin et al., 1996). Wignall and Newton (1998) applied this concept to Jurassic black shales from Britain, and were able to match small mean diameters (2–3 μm) and narrow size distributions to finely laminated black shales that lacked any sign of benthic life and were presumably deposited under anoxic bottom waters. They also found that samples that showed some evidence of bioturbation and were probably deposited under dysoxic conditions typically had mean framboid diameters in excess of 5 μm as well as broad size distributions.

Multiple samples through the Devonian New Albany Shale, the unit that hosts three of our pyritic lag examples, typically show mean framboid diameters in excess of 5 μm , and broad size distributions (unpublished data). This indicates that pyrite framboids formed within the surface sediment and under dysoxic bottom waters. Within these black shale samples one also finds clear evidence that pyrite framboids were reworked and concentrated into thin laminae (~10–50 μm thick) by bottom currents (unpublished petrographic observations), a result that agrees with the observation of abundant evidence for sediment reworking and erosion at the millimeter to meter scale throughout the Devonian black shale succession (Schieber, 1998a, b; Schieber and Lazar, 2004). This observation also explains why our black shale samples typically show degree of pyritization (DOP) values that are considered indicative of anoxic conditions (Raiswell et al., 1988), in spite of showing bioturbation in many instances (Schieber, 2003). The DOP is defined as the ratio between iron actually in pyrite and the iron that can potentially be converted to pyrite, and a value in excess of 0.75 is considered indicative of anoxic conditions (Raiswell et al., 1988). Our Devonian black shale samples typically have DOP values in excess of 0.75 (Schieber, 2001), but mechanical iron enrichment by winnowing of pyrite framboids substantially raised the amount of pyrite bound iron and thus the DOP. Consequently, high DOP values of Devonian shales associated with the studied lags are an artifact and not at all indicative of anoxic conditions. Based on the above observations it appears thus that bottom waters during Devonian black shale deposition were rarely if ever anoxic, a conclusion that is echoed by Sageman et al. (2003) in a geochemical study of several other Devonian black shale units from the eastern US.

Average terrigenous clastic sediments only contain up to a few percent reactive iron in the form of iron oxyhydroxide coatings on terrigenous grains (Carroll, 1958; Berner, 1969), and it is this iron component that is available for sedimentary pyrite formation. Sea water itself contains only very little iron in solution (~2 ppb; Drever, 1982) and is thus not a feasible iron source for substantial iron enrichment and marcasite formation. The described

lag deposits contain up to 40% (by volume) iron sulfides (Fig. 3A) and require an alternative mechanism for iron enrichment. Detrital pyrite grains in these lags (framboids, pyritized burrow tubes, pyrite-filled algal cysts, and irregular pyrite concretions) also are observed in the underlying shales, and therefore intermittent erosion and reworking of these shales provide a simple mechanism for removal of clays and concentration of quartz, phosphatic debris, and iron sulfide grains in the residuum. Iron enrichment in these lags is therefore a consequence of stratigraphic condensation and negative net sedimentation rates.

7. Redistribution of iron

After mechanical enrichment, however, a portion of the sulfide iron has to be remobilized to allow formation of marcasite overgrowth and pore filling cement. This requires that a portion of the preexisting sulfide grains be destroyed, either wholly or partially, in order to supply dissolved (Fe^{2+}) or readily soluble (e.g., $Fe(OH)_3$) iron for new iron sulfide growth.

Corrosion features like those shown in Figs. 1–3 indicate that marcasite precipitation is preceded by etching and partial dissolution of pre-existing iron sulfide grains. The fact that successive generations of marcasite can be separated by dissolution features (Fig. 1) indicates that pore water conditions oscillated between conditions that promoted iron sulfide dissolution and conditions favorable for marcasite deposition. Corrosion attests to intermittent grain dissolution, most likely by iron sulfide oxidation (Eq. (1)):

$$FeS_2 + 3.5O_2 + H_2O \rightarrow Fe^{2+} + 2SO_4^{2-} + 2H^+. \quad (1)$$

The reaction in Eq. (1) produces acidity and dissolved ferrous iron. Further oxidation of ferrous to ferric iron leads to formation of iron hydroxide and production of further acidity:

$$Fe^{2+} + 0.25O_2 + 2.5H_2O \rightarrow Fe(OH)_3 + 2H^+. \quad (2)$$

Thus, oxidation of iron sulfides causes formation of iron hydroxides and substantial lowering of pH. The newly formed iron hydroxides would form coatings on surface sediment grains (Berner, 1969) and would not diminish the overall iron enrichment of the surficial sediment layer. A sufficiently large drop of pore water pH would also promote large pore-water concentrations of dissolved ferrous iron (Fe^{2+}) (Maynard, 1983, p. 43).

8. Formation of marcasite

In order to form within sediments, both pyrite and marcasite require reducing pore waters, H_2S production, and a source of iron. An essential guidepost for thinking about marcasite in sedimentary environments has been experiments conducted by Murowchick and Barnes (1986), Schoonen and Barnes (1991a, b), and Benning et al. (2000). These experiments consistently indicate that marcasite formation is strongly favored over pyrite at low pH values (approximately 4–5), and also that low-pH marcasite growth is substantially faster than pyrite growth at higher pH, resulting in coarse crystalline marcasite vs. fine crystalline pyrite (Schoonen and Barnes, 1991b).

As discussed above, when iron sulfides are oxidized pore-water pH will drop substantially and high concentrations of dissolved Fe^{2+} are likely. All that is needed at that point is a source of hydrogen sulfide, such as from underlying or overlying organic-rich sediments, to cause rapid precipitation of marcasite.

9. Potential examples of marcasite formation via pyrite oxidation

Modern examples: Two recent reports of sedimentary pyrite–marcasite associations (Bush et al., 2004; Falconer et al., 2006) suggest that pyrite oxidation may indeed be a mechanism for marcasite formation in sediments. Falconer et al. (2006) describe diagenetic marcasite in conglomerates from a Pliocene nonmarine lignite succession in New Zealand, where marcasite occurs overgrowing and replacing framboidal pyrite. Marcasite is closely associated with organic matter and is reported to replace and overgrow earlier formed pyrite. Field relations and textural studies indicate that it is of recent authigenic origin. Falconer et al. (2006) did not propose that marcasite might be a direct consequence of the oxidation of pre-existing pyrite, but just as in our Devonian lag deposits, the boundaries between pyrite and marcasite are irregular, there are atoll structures and porous cores after pyrite framboids, and pyrite grains with surficial patches of iron oxides. Collectively these features can be interpreted as a result of intermittent pyrite oxidation and subsequent marcasite formation. Such an origin would be fully

consistent with climate-related fluctuations of groundwater levels that are common in terrestrial sedimentary deposits.

Formation of diagenetic marcasite also has been observed in organic-rich Holocene muds from a coastal backswamp in Australia (Bush et al., 2004). These marine to freshwater-brackish sediments contain early diagenetic pyrite throughout, but marcasite only occurs in association with fresh-water-brackish sediments. Marcasite overgrows cores of earlier formed pyrite with irregular boundaries. Bush et al. (2004) assumed continuously anaerobic conditions for the deposition of these sediments and did not consider the alternative of marcasite formation via intermittent pyrite oxidation. As long as only a fraction of the original organic matter is destroyed by intermittent oxidation such an oxidation event would be hard to detect and would require a very careful study of organic petrology for verification. What is currently known about these sediments is fully consistent with the premise that intermittent partial oxidation of sedimentary pyrite triggered lowering of pH and marcasite formation. In coastal settings, lowering of sea level typically induces deposition of freshwater-dominated sediments, and climate-related fluctuation of water levels (e.g., due to a drought) may well have resulted in intermittent oxidation and marcasite formation.

9.1. An ancient example

The Black Island Member of the Winnipeg Formation (Ordovician of Saskatchewan), a strongly bioturbated shallow marine sandstone unit with evidence for episodic wave reworking, contains coated iron sulfide grains with an oolitic texture and interspersed cortices of pyrite and marcasite. These coated iron sulfide grains are built on cores that represent reworked marcasite-mineralized borrows (Schieber, 2002) and involved intermittent episodes of tractional reworking, grain abrasion, reburial, and precipitation of further concentric laminae (Schieber and Riciputi, 2005). They formed as primary diagenetic precipitates under shallow burial conditions. Sulphide-coated grains formed during intervals of maximum sediment starvation, when organic matter was enriched in surface sediments, and rare storm waves intermittently reworked the surface sediment.

Alternate laminae of pyrite and marcasite within these grains point to substantial fluctuations in pore water pH, driven by intermittent oxidation of previously formed iron sulphides. SEM studies of these grains show corrosion pits in iron sulphide cortices that are infilled by pyrite or marcasite, and closely resemble corrosion features illustrated from Devonian pyritic lags. These corrosion features, together with evidence of mechanical reworking, support a scenario in which partial oxidation of reworked iron sulfides provided the iron for the growth of new sulfide cortices, as well as low pH for the formation of marcasite. Some stratigraphic horizons contain up to volume 40% iron sulphide grains and indicate negative net sedimentation to facilitate geochemical "reworking" of iron.

9.2. Environmental parameters

Whereas oxidation of detrital pyrite furnishes soluble iron for renewed iron sulfide growth, as well as low-pH conditions for marcasite formation, the winnowed lags are unlikely to contain much organic matter to support reducing conditions and H_2S production, the other requirements for iron sulfide precipitation. These latter conditions could, for example, be produced by upward diffusion of H_2S and dissolved organic matter from underlying shales. In this way pore-water oxygen in the lag could be eliminated by aerobic bacteria, iron hydroxides would buffer H_2S, and iron could be mobile in an anoxic and nonsulfidic environment (Berner, 1969, 1981). Alternatively, we could envision that organic-rich sediments blanketed these sulfidic lags during intervening low-energy intervals, caused an upward shift of the redox boundary, moved the lags into the sulfate reduction zone, and allowed formation of new iron sulfides.

Whether pH values necessary for marcasite formation were reached also may have depended on the overall iron sulfide concentration in the lag. High-sulfide lags were probably more likely to force sufficiently low pH values than lags with low amounts of iron sulfide grains. In the latter case pyrite, rather than marcasite may form in pore spaces and as overgrowths on iron sulfide grains. In the studied examples, recognition of newly grown marcasite is comparatively easy. However, whether a given pyrite grain resulted from marcasite inversion or whether it formed because the pH was unsuitable for marcasite growth requires additional textural clues, such as petrographic criteria described by Murowchick (1992).

Considering that oxygenated bottom waters seem to be essential for marcasite formation, and taking into account the generally small rates of sediment accumulation in black shales, one must wonder what allowed our sulfidic lags to "survive" at the seafloor until they were buried by organic-rich muds. One possible explanation is that benthic fluff layers were an important factor in the preservation of sulfidic lag deposits. In the modern, settling of a mixture of mucus, sedimentary organic matter, and fine-grained terrigenous matter can form benthic flocculent (fluff) layers (Pilskaln and Pike, 2001; Laima et al., 2002). These fluff deposits that can range in thickness from a few millimeters to more than 10 cm are cohesive and gelatinous, and usually also contain mucus producing polychaete worms (Laima et al., 2002). Due to their organic content the biological oxygen demand in these layers is so strong that the redox boundary moves up into the fluff layer soon after deposition (Laima et al., 2002). Such organic-rich fluff blankets probably could have settled on our sulfidic lags following reworking events, effectively protecting them from prolonged oxidation.

In this context, oxidation of pyritic lags and the attendant low-pH conditions that allowed marcasite formation should have been short-lived transient events. Because under low temperature experimental conditions marcasite has been shown to grow as much as 5 μm a week under low-pH conditions (Schoonen and Barnes, 1991b), short lived oxidation events (several months to a few years?) and transient low-pH conditions may well have sufficed to generate the marcasite observed in our lags.

Iron sulfide formation in sediments requires organic matter to drive bacterial sulfate reduction and H_2S supply. Using sulfate reduction equations proposed by Canfield and Raiswell (1991), one realizes that it requires approximately 5 cm^3 of pure organic matter (such as lactate, ethanol, acetate, formaldehyde, etc.) to precipitate 1 cm^3 of FeS_2 (pyrite or marcasite). In order to produce a 5-cm-thick lag with 40 vol% pore filling marcasite one would need at a minimum a 10-cm-thick layer of the aforementioned pure organics. If one considers that benthic fluff layers consist of water to a large degree, and if we also factor in that only a fraction of the organic matter will be utilized for sulfate reduction, it seems that high surface productivity is desirable in order to maintain a fluff blanket that can support sulfate reduction at the levels needed for rapid and extensive marcasite precipitation.

10. A model for marcasite cemented lags

The above discussion of marcasite bearing sediments of various ages in the context of necessary conditions for marcasite formation, and iron sulfide preservation suggests a logical sequence of events for the formation of pyritic lags with a marcasite component (Fig. 5). In the first step, coarse particles and sedimentary pyrite have to be winnowed from the underlying sediment (Fig. 5A, B). This could for example be accomplished due to wave reworking after lowering of sea level, or incrementally as a consequence of reworking by unusually powerful storms.

Lag formation is followed by the onset of pyrite oxidation and lowering of pH. Pore waters become enriched in dissolved iron, and part of the liberated iron may form oxide crusts on sediment grains (Fig. 5B). Because sediments are heterogenous by nature, diagenetic processes are subject to the chemical conditions at the pore space level and do not occur uniformly across an entire layer. Much of what happens at the pore space level depends on how much organic matter is present, how easily oxygen can diffuse down to that location (may vary due to presence or absence of internal clay drapes, etc.), and how active microbial decay operates as a consequence. So, whereas in one pore space we may have just enough oxygen for active pyrite oxidation, lowering of pH, and rising dissolved iron concentrations, higher oxygen concentrations in a pore space a few millimeters or centimeters away may promote deposition of iron hydroxide coatings instead (Fig. 5B′). Areas within the lag that contain dissolved iron and have low pH will see the onset of marcasite formation if there is an influx of hydrogen sulfide, either from decay of organic material within the lag, or from underlying carbonaceous muds. Marcasite will start to overgrow previously corroded pyrite grains, as well as replacing previously formed iron hydroxide crusts (Fig. 5C′). In order for substantial marcasite growth to occur the supply of dissolved iron has to be sustained for some time (probably at least weeks to months). This would imply that within the lag, pyrite oxidation would have to occur simultaneous with marcasite precipitation, but at different locations. Alternatively, the process could involve an initial stage of pyrite oxidation with formation of abundant iron hydroxide crusts, and a second stage of marcasite formation under anoxic conditions where the iron hydroxide crusts are dissolved again and "fuel" the rapid growth of marcasite cements.

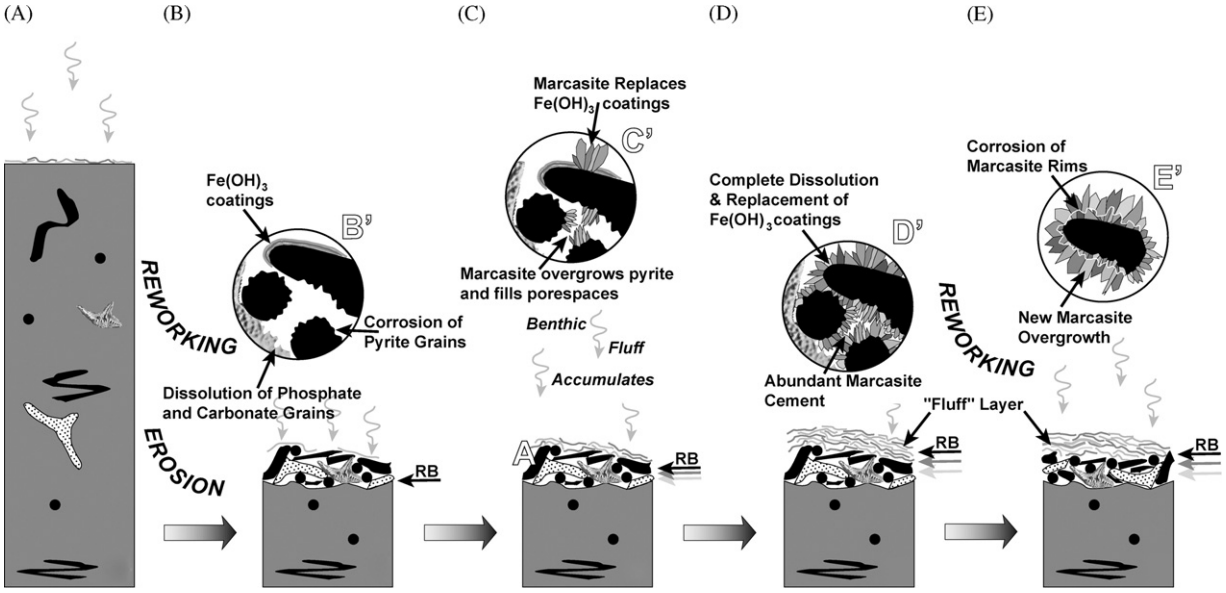

Fig. 5. Schematic summary of marcasite formation in Devonian pyritic lags. (A) Dysaerobic black shale accumulation. Black shale matrix in medium gray. Other features shown are pyrite-filled algal cysts (small black circles), pyritized burrows (irregular black lines), fish bones (stippled), and conodonts. Organic-rich detritus (benthic fluff) is settling on the sediment surface. (B) Reworking and erosion removes two-thirds of the original shale section, and coarse particles (''other features'' in A) now form a lag at the surface. The redox boundary (RB) is at the base of the lag. (B′) A pore space in the lag that shows pyrite particles (black) and the edge of a conodont. The waters contain oxygen and cause corrosion of pyrite surfaces, an increase in dissolved iron, and local formation of iron hydroxide coatings. The lowering of pH due to pyrite oxidation causes dissolution of conodont apatite as well as of carbonate grains (not shown). Benthic fluff starts to accumulate on the lag. (C) Continued accumulation of benthic fluff causes a gradual shift towards anoxic pore waters and the redox boundary (RB) starts to migrate upwards through the lag. (C′) Marcasite starts to precipitate on corroded pyrite grains and replaces previously formed iron hydroxide coatings. (D) Marcasite precipitation continues as the redox boundary migrates upwards towards the thickening fluff layer. (D′) Gradually pore spaces fill with marcasite cement and early formed iron hydroxide coatings have been dissolved or replaced. (E) If the lag is reworked again (e.g., due to a major storm), coarse particles are transported and winnowed. After low energy conditions return, the processes shown in B through D (oxidation, corrosion, marcasite precipitation) are repeated until the redox boundary has again moved into the fluff layer. (E′) Detail of a marcasite encrusted pyrite grain. Part of the grains' marcasite coating was formed prior to the second reworking event and has been corroded (white line). A second layer of marcasite has formed on the corroded surface.

The buildup of benthic fluff is probably an essential ingredient for prolonged iron sulfide survival beneath oxygen bearing bottom waters. Aerobic decay of its organic component reduces the oxygen availability to the lag beneath it, and allows for anoxic/nonsulfidic conditions (Berner, 1981) that facilitate iron migration to sites of marcasite precipitation. Over time this will cause the redox boundary to gradually move upwards through the lag (Fig. 5C) and eventually move into the fluff blanket itself (Fig. 5D) (Laima et al., 2002). At that point no more sulfide oxidation is possible in the lag, pH will rise, and no more marcasite formation will occur. It seems reasonable, therefore, to presume that there is only a comparatively short time span during which marcasite formation can occur in the proposed scenario.

The observation of multiple episodes of iron sulfide corrosion/oxidation in several samples suggests subsequent reworking and/or intermittent removal of the benthic fluff blanket (Fig. 5E, E′). Under those conditions we should expect to see more extensive marcasite cementation because they allow the lag to go through multiple cycles of re-oxidation and marcasite precipitation.

11. Implications

Finding marcasite in the marine lag deposits described here opens up a number of questions that warrant examination in more detail. For example, there is the notion that reworked iron sulfides in marine lags require that such lags form in association with anoxic bottom waters. The Leicester

Pyrite Bed is probably one of the best publicized examples, and Baird and Brett (1991) have provided us with a wealth of sedimentologic and petrographic detail of this particular occurrence. Because they needed to provide a plausible explanation for the preservation of so much pyrite at the seafloor, it seemed reasonable to explain this lag as a result of reworking from internal waves that traveled along the pycnocline of a stratified basin with anaerobic bottom waters. While this model ensures seafloor survival of detrital pyrite, discovering marcasite in these lags poses a problem. Given what we currently know about the conditions for marcasite formation (Murowchick and Barnes, 1986; Schoonen and Barnes, 1991a, b; Benning et al., 2000), textural details (corrosion) suggest that such lags have experienced one or more episodes of iron sulfide re-oxidation (Fig. 1D). In view of the alkaline pH in overlying seawater, rapid oxygenation probably offers the best chance to depress pore water pH to the levels needed for marcasite formation. Thus, while internal waves traveling along pycnoclines may well be responsible for the formation of certain pyritic lags in the rock record, once these lags contain secondary marcasite alternative explanations have to be explored. The need for a pH drop to form marcasite seems to call for oxidation of iron sulfides. This mode of formation eliminates the need for internal waves and a stratified basin, and also allows us to place lag formation at a shallower water depth, such as possibly storm wave base.

Sea-level drop produces erosion surfaces that are commonly known as sequence boundaries and are often covered by residual lags (Van Wagoner et al., 1988). After sea-level drop for example, such lags will form on now sub-aerially exposed shallow marine sediments, as well as on offshore shallow marine sediments. However, whereas pyrite-rich lags in the shallow marine/submarine realm may be preserved and contain marcasite as a consequence of intermittent pyrite re-oxidation, sub-aerially exposed pyrite-rich lags will be fully oxidized and all that remains of the pyrite will be an iron oxide crust on lag particles. Should the latter type of lag be covered with marine sediments during the next transgression, these iron oxides most likely will be converted to pyrite due to H_2S supply from overlying sediments (Schieber and Riciputi, 2004). There will, be, however, no opportunity to produce the low-pH conditions needed for marcasite formation. Thus, a lateral change in sequence boundary lags from marcasitic to non-marcasitic potentially could be used to map shoreline position during maximum regression. Marcasitic lags would indicate deposition seaward of the shoreline, whereas nonmarcasitic lags would indicate deposition landward of the shoreline. While all of this may be irrelevant in sandy successions where shoreline position is marked by littoral facies (Reineck and Singh, 1980), it could be very valuable in mudstone-dominated successions that lack sandy shoreline facies (Walker and Harms, 1971).

Following the above line of reasoning, one also might hypothesize that the marcasite to pyrite ratio of ancient marine pyritic lags could be used as a measure of relative bottom water oxygenation (better oxygenation with increasing ratio). This approach could be used to establish gradients within specific stratigraphic levels, or might be used to establish fluctuations through time from lags within a stratigraphic section or a drill core.

With EBSD we now have a powerful tool to identify marcasite as small grains in its textural context, and this gives us an opportunity to re-examine the occurrence and distribution of pyrite and marcasite in the rock record. Although it was long presumed that marcasite in older rocks has inverted to pyrite, the rocks examined in this study are in excess of 350 m.y. old and still contain well-preserved marcasite. This opens up the possibility that identifiable marcasite may be found much further back in the rock record, potentially changing our perceptions of prevailing conditions and processes. Depending on how far back in geologic history marcasite is preserved, it might even provide us with a new angle for evaluating the ever contentious oxygenation state of the Precambrian atmosphere (Kasting, 1993; Pavlov et al., 2003; Bekker et al., 2004).

Upon further study we may also find that re-oxidized pyritic lags are not the only scenario that gives rise to marcasite. Mudstones, for example, contain the bulk of sedimentary iron sulfides. If some of it were marcasite it surely would be illuminating and might prompt us to revise our views of early mudstone diagenesis.

Finally, given all the implications arising from discovering marcasite in ''unlikely'' places, we also need to make sure that our pyrite re-oxidation model for sedimentary marcasite actually applies to the majority of occurrences in the rock record. Therefore we need to examine a broad range of occurrences for textural and geochemical clues to their origin, and in addition conduct experiments

that test whether sedimentary marcasite would indeed form under the conditions envisioned here.

12. Conclusion

Textural observations on pyritic lags from the Late Devonian of the eastern US suggest that intermittent oxidation of detrital pyrite provides a mechanism for secondary marcasite formation. Pyrite oxidation promotes lowering of pH, brings reduced iron into solution, and in the presence of H_2S creates favorable conditions for marcasite formation. Recognition of marcasite in ancient sedimentary rocks may shed new light on a variety of issues related to the oxygenation state of seawater, the placement of shoreline positions in otherwise mudstone-dominated successions, and provide mineralogical constraints on geochemical processes operating during early diagenesis.

Acknowledgments

Research on Devonian black shales has for many years been supported by the Petroleum Research Fund. Acknowledgment is made to the donors of the Petroleum Research Fund, administered by the American Chemical Society (Grants 30774-AC8, 25134-AC2, 38523-AC8). An NSF instrumentation grant (EAR-0318769) provided funds for the acquisition of an analytical ESEM with EDS and EBSD capabilities that were used for this research. Thanks go to Gabe Fillipelli for encouraging me to further develop my musings on marcasite in sediments and to present my ideas at session OS16 (Authigenic Mineral Formation in the Marine Environment: Pathways, Processes, and Products) at the 2004 AGU meeting in San Francisco, and to Craig Glenn and Gabe Fillipelli for undertaking the editing of this special volume.

References

Baird, G.C., Brett, C.E., 1991, Submarine erosion on the anoxic sea floor: stratinomic, palaeoenvironmental, and temporal significance of reworked pyrite–bone deposits. In: Tyson, R.V., Pearson, T.H. (Eds.), Modern and Ancient Continental Shelf Anoxia: Geological Society [London], Special Publication No. 58, pp. 233–257.

Bannister, F.A., 1932. The distinction of pyrite from marcasite in nodular growths. Mineralogical Magazine 23, 179–187.

Bekker, A., Holland, H.D., Wang, P.L., Rumble, D., Stein, H.J., Hannah, J.L., Coetzee, L.L., Beukes, N.J., 2004. Dating the rise of atmospheric oxygen. Nature 427, 117–120.

Benning, L.G., Wilkin, R.T., Barnes, H.L., 2000. Reaction pathways in the Fe–S system below 100 °C. Chemical Geology 167, 25–51.

Berner, R.A., 1969. Migration of iron and sulfur within anaerobic sediments during early diagenesis. American Journal of Science 267, 19–42.

Berner, R.A., 1981. A new geochemical classification of sedimentary environments. Journal of Sedimentary Petrology 51, 359–365.

Berner, R.A., 1984. Sedimentary pyrite formation: an update. Geochimica et Cosmochimica Acta 48, 605–615.

Bohacs, K.M., 1998. Contrasting expressions of depositional sequences in mudrocks from marine to non-marine environs. In: Schieber, J., Zimmerle, W., Sethi, P. (Eds.), Shales and Mudstones, 1. Basin Studies, Sedimentology and Paleontology, Schweizerbart'sche Verlagsbuchhandlung, Stuttgart, pp. 33–78.

Bush, R.T., McGrath, R., Sullivan, L.A., 2004. Occurrence of marcasite in an organic-rich Holocene estuarine mud. Australian Journal of Soil Research 42, 617–621.

Canfield, D.E., Raiswell, R., 1991. Pyrite formation and fossil preservation. In: Allison, P.A., Briggs, D.E. (Eds.), Taphonomy: Releasing the Data Locked in the Fossil Record. Plenum Press, New York, pp. 337–387.

Carroll, D., 1958. Role of clay minerals in the transportation of iron. Geochemica et Cosmochimica Acta 14, 1191–1206.

Drever, J.I., 1982. The Geochemistry of Natural Waters. Prentice-Hall, Englewood Cliffs, NJ, 388pp.

Falconer, D.M., Craw, D., Youngson, J.H., Faure, K., 2006. Gold and sulphide minerals in tertiary quartz pebble conglomerate gold placers, Southland, New Zealand. Ore Geology Reviews 28, 525–545.

Foslie, S., 1950. Supergene marcasite replacing pyrrhotite. Norsk Geologisk Tidsskrift 28, 144–150.

Jowett, E.C., Roth, T., Rydzewski, A., Oszczepalski, S., 1991. "Background" delta 34S values of Kupferschiefer sulphides in Poland; pyrite–marcasite nodules. Mineralium Deposita 26, 89–98.

Kasting, J.F., 1993. Earth's early atmosphere. Science 259, 920–926.

Krumbein, W.C., Garrels, R.M., 1952. Origin and classification of chemical sediments in terms of pH and oxidation–reduction potentials. Journal of Geology 60, 1–33.

Laima, M., Maksymowska-Brossard, D., Sauriau, P.-G., Richard, P., Girard, M., Gouleau, D., Joassard, L., 2002. Fluff deposition on intertidal sediments: effects on benthic biota, ammonium fluxes and nitrification rates. Biogeochemistry 61, 115–133.

Maynard, J.B., 1983. Geochemistry of Sedimentary Ore Deposits. Springer, New York, 305pp.

Maynard, J.B., Lauffenburger, S.K., 1978. A marcasite layer in prodelta turbidites of the Borden Formation (Mississippian) in eastern Kentucky. Southeastern Geology 20, 47–58.

Murowchick, J.B., 1992. Marcasite inversion and the Petrographic determination of Pyrite Ancestry. Economic Geology 87, 1141–1152.

Murowchick, J.B., Barnes, H., 1986. Marcasite precipitation from hydrothermal solutions. Geochimica et Cosmochimica Acta 50, 2615–2629.

Nayar, K.V., 1946. Marcasite in Travancore lignite. Current Science 15, 229.

Newhouse, W.H., 1925. Paragenesis of marcasite. Economic Geology 26, 54–66.

Pavlov, A.A., Hurtgen, M.T., Kasting, J.F., Arthur, M.A., 2003. Methane-rich Proterozoic atmosphere? Geology 31, 87–90.

Pilskaln, C.H., Pike, J., 2001. Formation of sedimentary laminae in the Black Sea and the role of the benthic flocculent layer. Paleoceanography 16, 1–19.

Prior, D.J., Boyle, A.P., Brenker, F., Cheadle, M.C., Day, A., Lopez, G., Peruzzo, L., Potts, G.J., Reddy, S.M., Spiess, R., Timms, N.E., Trimby, P.W., Wheeler, J., Zetterstrom, L., 1999. The application of electron backscatter diffraction and orientation contrast imaging in the SEM to textural problems in rocks. American Mineralogist 84, 1741–1759.

Raiswell, R., Buckley, F., Berner, R.A., Anderson, T.F., 1988. Degree of pyritization of iron as a paleoenvironmental indicator of bottom water oxygenation. Journal of Sedimentary Petrology 58, 812–819.

Read, H.W., Cook, A.C., 1969. Note on coals containing marcasite plant petrifactions, Yarrunga creek, Sydney Basin, New South Wales. Journal and Proceedings of the Royal Society of New South Wales 102, 197–199.

Reineck, H.E., Singh, I.B., 1980. Depositional Sedimentary Environments. Springer, New York, 549pp.

Rickard, D., Schoonen, M.A.A., Luther, G.W., 1995. Chemistry of iron sulfides in sedimentary environments. In: Vairavamurtry, M.A., Schoonen, M.A.A. (Eds.), Geochemical Transformations of Sedimentary Sulfur. ACS Symposium Series 612, Washington, pp. 165–193.

Rykart, R., 1983. "Gilded" petrifications; formation of pyrite and marcasite in bituminous shale. Mineralien Magazin 7, 280–284.

Sageman, B.B., Murphy, A.E., Werne, J.P., Ver Straeten, C.A., Hollander, D.J., Lyons, T.W., 2003. A tale of shales: the relative roles of production, decomposition, and dilution in the accumulation of organic-rich strata, Middle-Upper Devonian, Appalachian basin. Chemical Geology 195, 229–273.

Schieber, J., 1998a. Sedimentary features indicating erosion, condensation, and hiatuses in the Chattanooga Shale of Central Tennessee: relevance for sedimentary and stratigraphic evolution. In: Schieber, J., Zimmerle, W., Sethi, P. (Eds.), Shales and Mudstones, vol. 1. Basin Studies, Sedimentology and Paleontology, Schweizerbart'sche Verlagsbuchhandlung, Stuttgart, pp. 187–215.

Schieber, J., 1998b. Developing a sequence stratigraphic framework for the Late Devonian Chattanooga shale of the southeastern US: relevance for the Bakken Shale. In: Christopher, J.E., Gilboy, C.F., Paterson, D.F., Bend, S.L. (Eds.), Eight International Williston Basin Symposium, Saskatchewan Geological Society Special Publication No. 13, pp. 58–68.

Schieber, J., 2001. Ways in which organic petrology could contribute to a better understanding of black shales. International Journal of Coal Geology 47, 171–187.

Schieber, J., 2002. The role of an organic slime matrix in the formation of pyritized burrow trails and pyrite concretions. Palaios 17, 104–109.

Schieber, J., 2003. Simple gifts and hidden treasures—implications of finding bioturbation and erosion surfaces in black shales. The Sedimentary Record 1, 4–8.

Schieber, J., Baird, G., 2001. On the origin and significance of pyrite spheres in Devonian black shales of North America. Journal of Sedimentary Research 71, 155–166.

Schieber, J., Lazar, R.O. (Eds.), 2004. Devonian black shales of the eastern US: new insights into sedimentology and stratigraphy from the subsurface and outcrops in the Illinois and Appalachian Basins. In: Field Guide for the 2004 Great Lakes Section SEPM Annual Field Conference. Indiana Geological Survey Open File Study 04-05, 90pp.

Schieber, J., Riciputi, L., 2004. Pyrite ooids in Devonian black shales record intermittent sea level drop and shallow water conditions. Geology 32, 305–308.

Schieber, J., Riciputi, L., 2005. Pyrite–marcasite coated grains in the Ordovician Winnipeg Formation, Canada: an intertwined record of surface conditions, stratigraphic condensation, geochemical "reworking," and microbial activity. Journal of Sedimentary Research 75, 905–918.

Schoonen, M.A.A., 2004. Mechanisms of sedimentary pyrite formation. In: Lyons, T.W. (Ed.), Sulfur Biogeochemistry—Past and Present. Geological Society of America Special Paper Paper #379, pp. 117–134.

Schoonen, M.A.A., Barnes, H.L., 1991a. Reactions forming pyrite and marcasite from solution. I. Nucleation of FeS_2 below 100 °C. Geochimica et Cosmochimica Acta 55, 1495–1504.

Schoonen, M.A.A., Barnes, H.L., 1991b. Reactions forming pyrite and marcasite from solution. II. Via FeS precursor below 100 °C. Geochimica et Cosmochimica Acta 55, 1505–1514.

Schwartz, A.J., Kumar, M., Adams, B.L., 2000. Electron Backscatter Diffraction in Materials Science. Springer, Berlin, 350pp.

Siesser, W.G., 1978. Petrography and geochemistry of pyrite and marcasite in DSDP Leg 40 sediments: initial reports of the deep sea drilling project. Supplement to Volumes 38, 39, 40, and 41, September. 1978, pp. 767–775.

Van Horn, F.R., Van Horn, K.R., 1933. X-ray study of pyrite of marcasite concretions in the rocks of the Cleveland, Ohio, quadrangles. American Mineralogist 18, 288–294.

Van Wagoner, J.C., Posamentier, H.W., Mitchum, R.M., Vail, P.R., Sarg, J.F., Loutit, T.S., Hardenbol, J., 1988. An overview of the fundamentals of sequence stratigraphy and key definitions. In: Wilgus, C.K., Hastings, B.S., Kendall, C.G.St.C., Posamentier, H.W., Ross, C.A., Van Wagoner, J.C. (Eds.), Sea-level Changes: An Integrated Approach. Society of Economic Paleontologists and Mineralogists. Special Publication No. 42, pp. 39–45.

Walker, R.G., Harms, J.C., 1971. The "Catskill Delta". A prograding muddy shoreline in central Pennsylvania. Journal of Geology 79, 381–399.

Wignall, P.B., Newton, R., 1998. Pyrite framboid 1 diameter as a measure of oxygen-deficiency in ancient mudrocks. American Journal of Science 298, 537–552.

Wiese, R.G., Powell, M.A., Fyfe, W.S., 1987. Spontaneous formation of hydrated iron sulfates on laboratory samples of pyrite- and marcasite-bearing coals. Chemical Geology 63, 29–38.

Wilkin, R.T., 2003. Sulfide minerals in sediments. In: Middleton, G.V. (Ed.), Encyclopedia of Sediments and Sedimentary

Rocks. Kluwer Academic Publishers, Dordrecht, pp. 701–703.

Wilkin, R.T., Barnes, H.L., 1997. Formation processes of framboidal pyrite. Geochimica et Cosmochimica Acta 61, 323–339.

Wilkin, R.T., Barnes, H.L., Brantley, S.L., 1996. The size distribution of framboidal pyrite in modern sediments: an indicator of redox conditions. Geochimica et Cosmochimica. Acta 60, 3897–3912.

Williams, M.L., Crossey, L.J., Jercinovic, M.D., Bloch, J.D., Karlstrom, K.E., Dehler, C.M., Heizler, M.T., Bowring, S.A., Goncalves, P., 2003. Dating sedimentary sequences; in situ U/Th–Pb microprobe dating of early diagenetic monazite and Ar–Ar dating of marcasite nodules; case study from Neoproterozoic black shales in the Southwestern US. Geological Society of America, Abstracts with Programs, vol. 35/6, 595pp.